



Gas Condensate Relative Permeability for Well Calculations

CURTIS H. WHITSON^{1,2}, ØIVIND FEVANG² and AUD SÆVAREID³

¹Norwegian University of Science and Technology, NTNU, Norway

²Pera a/s

³Statoil a/s

(Received: 5 October 2001; in final form: 28 October 2002)

Abstract. This paper addresses several issues related to the modeling and experimental design of relative permeabilities used for simulating gas condensate well deliverability. Based on the properties of compositional flow equations, we make use of the fact that relative permeability ratio k_{rg}/k_{ro} is a purely thermodynamic variable, replacing saturation, when flow is steady-state. The key relation defining steady-state flow in gas condensate wells is relative permeability k_{rg} as a function of k_{rg}/k_{ro} . Consequently, determination of saturation and k_r as a function of saturation is not important for this specific calculation. Once the $k_{rg} = f(k_{rg}/k_{ro})$ relationship is experimentally established and correlated with capillary number (N_c), accurate modeling of condensate blockage is possible. A generalized model is developed for relative permeability as the function of k_{rg}/k_{ro} and capillary number. This model enables us to link the ‘immiscible’ or ‘rock’ curves with ‘miscible’ or ‘straight-line’ curves by a *transition function* dependent on the capillary number. This model is also extended to the case of high-rate, inertial gas flow within the steady-state condensate blockage region and locally at the wellbore. We have paid particular attention to the effect of hysteresis on the relation $k_{rg} = f(k_{rg}/k_{ro})$, based on our observation that many repeated cycles of partial/complete imbibition and drainage occur in the near-well region during the life of a gas condensate well. Finally, the composite effect of condensate blockage is handled using a ‘Muskat’ pseudopressure model, where relative permeabilities are corrected for the positive effect of capillary number dependence and the negative effect of inertial high velocity flow. Special steady-state experimental procedures have been developed to measure k_{rg} as a function of k_{rg}/k_{ro} and N_c . Saturations, though they can be measured, are not necessary. An approach for fitting steady-state gas condensate relative permeability data has been developed and used for modeling relative permeability curves.

Key words: gas condensate, condensate blockage, steady-state flow, well performance, relative permeability.

Nomenclature

A	cross-sectional area to flow; constant in Chierici k_{ro} correlation.
B	constant in Chierici k_{rg} correlation.
B_{gd}	dry-gas FVF.
c_{g1}, c_{g2}, c_{g3}	constants in Arco k_{rg} correlation.
c_{o1}, c_{o2}, c_{o3}	constants in Arco k_{ro} correlation.
f_i	immiscibility factor.
k	absolute water permeability (md).
k_r	relative permeability, relative to <i>absolute</i> permeability.
k_{rg}	relative permeability to gas.
k_{rgI}	‘immiscible’ ($N_c = 0$) relative permeability to gas.
k_{rgM}	‘miscible’ ($N_c = \infty$) relative permeability to gas.

k_{rg}^o	gas relative permeability at S_{wi} .
k_{rg}	average gas relative permeability of immiscible and miscible value at $\alpha N_c = 1$.
k_{ro}	relative permeability to oil.
k_{ro}^o	oil relative permeability at S_{wi} .
k_{rg}/k_{ro}	gas-oil relative permeability ratio.
L	core length; constant in Chierici correlation.
M	constant in Chierici correlation.
n	exponent in equation for immiscibility factor.
n_g	exponent in equation for k_{rg} immiscibility factor.
n_o	exponent in equation for k_{ro} immiscibility factor.
N_c	P in $\Delta P_{viscous}$.
N_{cg}	capillary number based on gas velocity = $v_{pg}\mu_g/\sigma_{go}$.
P	pressure.
P_p	pseudopressures, Eq. (2.15).
P_v	viscous (Darcy) pressure drop.
P_{vg}	gas viscous pressure drop.
P_{vo}	oil viscous pressure drop.
P_{wf}	wellbore flowing pressure.
ΔP	pressure drop.
P_c	capillary pressure.
PV_{inj}	pore volumes injected.
q	flow rate.
q_g	core gas rate.
q_{inj}	injection rate evaluated at the pressure of the injection pump.
r	radius.
r_e	external boundary radius.
r_{ref}	reference $k_r(S)$ curve.
r_w	wellbore radius.
R_g	gas saturation variable.
R_o	oil saturation variable.
s	relative oil volume $\equiv v_o/(v_o + v_g) = v_{ro}$.
S	saturation.
S_g	gas saturation.
S_{gc}	critical oil saturation.
S_{ge}	effective gas saturation.
S_o	oil saturation.
S_{oc}	critical (residual-to-gas) oil saturation.
S_{oe}	effective oil saturation.
S_w	water saturation.
S_{wi}	irreducible water saturation.
v	volume.
v_{ro}	relative oil volume $\equiv v_o/(v_o + v_g) = s$.
V	velocity.
V_g	Darcy gas velocity.
V_p	pore velocity.
V_{pg}	gas pore velocity.
Z	gas Z-factor.

Greek Symbols

α	scaling parameter for N_c .
α_g	gas scaling parameter for N_c .

α_o	oil scaling parameter for N_c .
β	inertial HVF coefficient.
β_{eff}	effective inertial HVF coefficient including effect of k_{rg} .
ξ	total mass concentration.
η	chemical potential.
λ	mobility.
λ_g	gas mobility.
λ_o	oil mobility.
ρ	mass density.
ρ_g	gas density.
μ	viscosity.
μ_g	gas viscosity.
μ_o	oil viscosity.
σ_{go}	interfacial tension (IFT).
ϕ	porosity.

1. Introduction

The typical chemical composition of a gas-condensate mixture is dominated by volatile components such as methane, and a rather ‘small’ amount of heavy hydrocarbon components (<15 mol-%), though these heavier components make up a considerably larger percentage of the liquid phase (‘retrograde condensate’) formed during pressure decrease below an upper dewpoint. For practically any retrograde condensate reservoir, the condensate saturation is, throughout most of the reservoir, so low that its mobility is much less than gas mobility and for practical purposes can be considered immobile. Nevertheless, this gas-dominated flow behavior is not at all correct in the vicinity of gas-condensate wells where condensate saturations often reach high values (>50%), and oil permeability may exceed gas permeability ($k_{rg}/k_{ro} < 1$).

Condensate blockage near the wellbore may reduce gas well deliverability appreciably, though the severity depends on a number of reservoir and well parameters. Condensate blockage *is* important if the pressure drop from the reservoir to the wellbore is a significant percentage of the total pressure drop from reservoir to delivery point (e.g. a surface separator) *at the time (and after) a well goes on decline*. Reservoirs with low-to-moderate permeability (<10–50 md) are often ‘problem’ wells where condensate blockage must be handled properly. Wells with high k_h products (>5–10,000 md-ft) are typically not affected by reservoir pressure drop because the well’s deliverability is constrained almost entirely by the tubing. In this case, condensate blockage is a *non-issue*.

As previously discussed by Fevang and Whitson (1996), gas-condensate flow and saturation distribution in gas condensate reservoirs can be classified into three categories: (1) a near-well region where the gas/oil flow is steady-state, the condensate saturation is high and results in a severe hysteresis behavior throughout the life of a well – experiencing hundreds of cycles of complete or partial imbibition and drainage; (2) in the bulk of the reservoir far-removed from the wells, a second region exhibits only gas flow at a somewhat reduced permeability, while the con-

densate saturation remains very low but increases in time, where this process can be treated as imbibition throughout the life of the reservoir; and (3) beyond region (2) where pressures are above the initial dewpoint and no condensate saturation is found. In this paper we do not consider the complex relative permeability behavior where, through water encroachment, the gas and/or retrograde condensate are trapped by aquifer water in quantities from 15–40 saturation percent, and where all three phase permeabilities can be significantly reduced.

In terms of *reservoir well performance*, the near-well behavior, determined by the near-well relative permeability functions, is the dominant factor. The far-removed region II of condensate accumulation has somewhat reduced gas relative permeability, but this effect is generally second-order regarding well performance. Trapped saturations and reduced water relative permeability in water encroachment domain can be important for reservoir performance, but has no direct effect on well performance prior to water breakthrough.

The purpose of this paper is to present an approximate approach to model gas condensate wells, which is based on the hypothesis of a dominant role of the near-well region and a steady-state flow within this region. The analysis of steady-state flow equations leads to a simple hydrodynamic formula similar to the Dupuit equation, relating flow rate with a ‘Muskat’ pseudopressure intergral. The pseudopressure integral contains thermodynamic functions and relative permeabilities.

To calculate thermodynamic functions we have obtained a closed thermodynamic system of equations (phase splitting the overall flowing composition), which are entirely independent of the hydrodynamic sub-system. Moreover, we have strictly shown that this thermodynamic system is monovariant, such that all the thermodynamic variables depend on pressure only.

The second parameter determining the pseudopressure integral is the relative permeability. To calculate k_r we have developed generalized models which are founded on the fundamental laws of flow behavior near gas condensate wells. This flow behavior is characterized by a condensate ‘blockage’ near the wellbore where gas relative permeability is reduced by the buildup of a significant *mobile* condensate saturation. Condensate blockage may reduce well deliverability appreciably, though the severity depends on a number of reservoir and well parameters.

The dependence of relative permeability on capillary number may also be important, particularly for rich condensates with high delivery pressures (i.e. high bottomhole flowing pressures when the well is on decline). Capillary number describes the relative balance of viscous and capillary forces ($N_c = \Delta p_{\text{viscous}}/P_c$, or $N_c = v_{\text{pg}}\mu_g/\sigma_{\text{go}}$). For small N_c , capillary forces dominate and traditional (‘immiscible’) relative permeability behavior is found. For large N_c , viscous forces dominate and relative permeabilities tend to approach straight lines or ‘miscible-like’ behavior. In our modeling approach, we correlate relative permeability using a generalized equation that consists of a traditional ‘immiscible’ (Corey-type (Brooks and Corey, 1966; Standing, 1975)) relation and a simple one-parameter correlation for capillary number dependence.

The relative permeability model we develop also considers scaling for the variation of endpoint saturations. Our heuristic approach is based on maintaining the fundamental relationship $k_{rg} = f(k_{rg}/k_{ro})$, independent of endpoint saturation.

The last part of this paper is devoted to the experimental determination of relative permeabilities for gas-condensate systems. According to theoretical analysis, it is readily shown that the relative permeability ratio k_{rg}/k_{ro} is a universal function of pressure if gas-condensate flow is steady-state. Hence, the ratio k_{rg}/k_{ro} is a thermodynamic variable and can then be obtained directly from PVT experiment (or PVT simulation). Moreover, because the measured data can be presented in the form $k_{rg} = f(k_{rg}/k_{ro})$ instead of $k_{rg}(S)$ and $k_{ro}(S)$, we do not require the measurement of saturation. The immiscible correlations are transformed from their traditional format of $k_r(S)$ to $k_{rg}(k_{rg}/k_{ro})$ in the fitting process. Once the correlation is fit to measured data, it is readily converted back to the form $k_r(S)$ needed in traditional reservoir modeling.

In 1942, Evinger and Muskat (1942) and Saevareid *et al.* (1999) already made the same observation that saturation measurements are not important for saturated oil well performance – where $k_{ro} = f(k_{rg}/k_{ro})$ is independent of S_o . This observation in gas condensate systems is particularly important because it provides a more accurate and consistent interpretation of data from various sources (laboratories, model studies, etc.). A plot $k_{rg} = f(k_{rg}/k_{ro})$ – for gas condensate reservoirs – highlights the relevant k_{rg}/k_{ro} range for the particular reservoir and provides a key tool for quantifying condensate blockage.

Thus, we concentrate on the steady-state flowing conditions found in the near-well region – typically up to 100 m away from the wellbore. Specifically, we try to use laboratory pressures (Saevareid *et al.*, 1999) and flow velocities similar to those experienced by wells *in a given field*. Relative permeability measurements are limited to the key data required to model flow behavior at these conditions – namely the relationship $k_{rg} = f(k_{rg}/k_{ro})$.

The results of our experimental and modeling work on relative permeability has been implemented in full-field reservoir simulation models using the concept of a generalized pseudopressure function. Well productivity calculations based on pseudopressure include the effects of condensate blockage, capillary number dependence of relative permeability, high-velocity ('non-Darcy') effects, and well geometry.

2. Theory of Steady-State Compositional Flow

2.1. GENERAL EQUATIONS OF COMPOSITIONAL FLOW

Let us examine the system of equations describing the flow of a two-phase multicomponent mixture in porous medium:

$$\phi \frac{\partial(\zeta^{(k)} \rho)}{\partial t} + \text{div}(V_g \phi (1-s) \rho_g c_g^{(k)} + V_o \phi s \rho_o c_o^{(k)}) = 0, \quad (k = 1, \dots, N) \quad (2.1)$$

$$U_g \phi (1 - s) = -\frac{k k_{rg}(s)}{\mu_g} \text{grad } P_g, \quad U_o \phi s = -\frac{k k_{ro}(s)}{\mu_o} \text{grad } P_o \quad (2.2)$$

$$\zeta^{(k)} = \frac{\rho_g c_g^{(k)}(1 - s) + \rho_o c_o^{(k)} s}{\rho_g(1 - s) + \rho_o s}, \quad (k = 1, \dots, N);$$

$$\rho = \rho_g(1 - s) + \rho_o s \quad (2.3)$$

$$\eta_g^{(k)}(P_g, c_g^{(1)}, \dots, c_g^{(N)}) = \eta_o^{(k)}(P_o, c_o^{(1)}, \dots, c_o^{(N)}),$$

$$(k = 1, \dots, N); \quad P_g = P_o + P_c(s) \quad (2.4)$$

$$\rho_g = \rho_g(P_g, c_g^{(1)}, \dots, c_g^{(N)}), \quad \rho_o = \rho_o(P_o, c_o^{(1)}, \dots, c_o^{(N)}) \quad (2.5)$$

$$\sum_{k=1}^N c_g^{(k)} = 1, \quad \sum_{k=1}^N c_o^{(k)} = 1 \quad (2.6)$$

where ϕ is the porosity; k is the permeability; $k_{rg}(s)$ and $k_{ro}(s)$ are the relative gas and condensate (oil) permeabilities; $P_c(s)$ is the capillary pressure; $\zeta^{(k)}$ is the total mass concentration of k th component in the system; $c_g^{(k)}$ is the mass concentration of k th component in gas; $c_o^{(k)}$ is the mass concentration of k th component in oil; ρ is the total density; ρ_g and ρ_o are the gas and the oil densities; μ_g and μ_o are the gas and oil viscosities; V_g and V_o are the true gas and oil flow velocities; P_g and P_o are the gas and oil pressures; $\eta_g^{(k)}$ and $\eta_o^{(k)}$ are the chemical potentials of k th component in gas and oil. s is not the traditional pore-volume saturation, but it represents the fraction of flowing mixture volume which is oil, $s \equiv v_{ro} = v_o/(v_o + v_g) = q_o/(q_o + q_g)$, where v_o and v_g are volumes of the following mixture.

Equation (2.1) is the mass conservation law written for each component; each Equation (2.2) is the Darcy law written for each fluid phase; Equation (2.3) are the definitions of the total concentration and total density; Equation (2.4) are the equilibrium conditions; Equation (2.5) are the equations of phase state.

Let the medium properties: ϕ , k , $k_{rg}(s)$, $k_{ro}(s)$ and $P_c(s)$ be known. Let the fluid viscosities be known too. Then system (2.1) – (2.6) consisting of $(3N + 8)$ equations contains $(3N + 8)$ variables: $\zeta^{(k)}$, $c_g^{(k)}$, $c_o^{(k)}$, ρ , ρ_g , ρ_o , U_g , U_o , P_g , P_o , s .

2.2. EQUATIONS OF STEADY-STATE COMPOSITIONAL FLOW

Let the flow be steady-state. Then the time-derivatives in (2.1) are zero. Hence, we obtain the following sub-system instead of (2.1):

$$\zeta^{(k)} = \zeta^{(k)0} = \text{const}, \quad (k = 1, \dots, N - 1) \quad (2.7a)$$

$$\text{div}(V_g \phi (1 - s) \rho_g c_g^{(k)} + V_o \phi s \rho_o c_o^{(k)}) = 0, \quad (k = 1, \dots, N) \quad (2.7b)$$

where $\zeta^{(k)0}$ is ‘initial’ total concentration, that is, some values given by the initial conditions. System (2.7a) contains only $(N - 1)$ equations, as only $(N - 1)$ initial

values $\zeta^{(k)0}$ are independent ($\sum_k \zeta^{(k)0} = 1$). A supplementary equation following from (2.1), $\rho = \rho^0 = \text{const}$, is not also independent, as it is the sum of (2.7a) from 1 to N .

Note that relationships (2.7a) mean that the total mixture composition remains constant during steady-state flow.

System (2.7), (2.2) – (2.6) contains now $(4N + 7)$ equations with $(3N + 8)$ variables. Such a system is overdetermined.

To the steady-state system be physically and mathematically correct, the following relation must be satisfied:

$$V_g = V_o \equiv V \tag{2.8}$$

which means that the true flow velocity is the same for both phases.

Then (2.7b) takes the form for any index k :

$$\begin{aligned} 0 &= \text{div}(V\phi[\rho_g c_g^{(k)}(1-s) + \rho_o c_o^{(k)}s]) \\ &= \text{div}(V\phi\zeta^{(k)}\rho) = \zeta^{(k)0}\rho^0 \text{div}(V\phi) \end{aligned}$$

or

$$\text{div}(V\phi) = 0 \tag{2.9}$$

Finally, the steady-state flow model of compositional flow represents a system which is split into a hydrodynamic and a thermodynamic sub-system.

The hydrodynamic sub-system:

$$\text{div}(V\phi) = 0, \quad V = -\frac{kk_{rg}(s)}{\phi(1-s)\mu_g} \text{grad}P, \quad V_o = V \tag{2.10}$$

The thermodynamic sub-system:

$$\zeta^{(k)} = \zeta^{(k)0} = \text{const}, \quad (k = 1, \dots, N - 1) \tag{2.11a}$$

$$\zeta^{(k)} = \frac{\rho_g c_g^{(k)}(1-s) + \rho_o c_o^{(k)}s}{\rho_g(1-s) + \rho_o s}, \quad (k = 1, \dots, N) \tag{2.11b}$$

$$\begin{aligned} \eta_g^{(k)}(P, c_g^{(1)}, \dots, c_g^{(N)}) &= \eta_o^{(k)}(P_o, c_o^{(1)}, \dots, c_o^{(N)}), \\ (k = 1, \dots, N); \quad P &= P_o + P_c(s) \end{aligned} \tag{2.11c}$$

$$\rho_g = \rho_g(P, c_g^{(1)}, \dots, c_g^{(N)}), \quad \rho_o = \rho_o(P_o, c_o^{(1)}, \dots, c_o^{(N)}) \tag{2.11d}$$

$$\sum_{k=1}^N c_g^{(k)} = 1, \quad \sum_{k=1}^N c_o^{(k)} = 1 \tag{2.11e}$$

This system contains in total $(3N + 7)$ equations with $(3N + 7)$ variables: $\zeta^{(k)}$, $c_g^{(k)}$, $c_o^{(k)}$, ρ_g , ρ_o , $V \equiv V_g$, V_o , $P \equiv P_g$, P_o , s . The system is correct.

2.3. UNIVERSAL RELATION BETWEEN RELATIVE PERMEABILITY RATIO AND SATURATION

Four important corollaries follow from the steady-state model:

$$\frac{k_{rg}\mu_o}{k_{ro}\mu_g} = \frac{(1-s)}{s}, \quad \text{if } P_g = P_o \quad (2.12a)$$

$$\frac{k_{rg}\mu_o}{k_{ro}\mu_g} = \frac{(1-s)}{s} \frac{dP_o}{dP}, \quad \text{if } P_g \neq P_o \text{ and the flow is 1D} \quad (2.12b)$$

and

$$\frac{k_{rg}}{\mu_g} + \frac{k_{ro}}{\mu_o} = \frac{k_{rg}}{(1-s)\mu_g}, \quad \text{in both cases} \quad (2.12c)$$

These relations are easy to prove. Let us examine ratio of two Darcy's velocities given by (2.2):

$$\frac{k_{rg}\mu_o \text{grad} P_g}{k_{ro}\mu_g \text{grad} P_o} = \frac{U_g(1-s)}{U_o s}$$

On the left-hand side, the gradients may be eliminated if the phase pressures are the same. If not, the ratio of gradients in 1D case equals dP_g/dP_o . On the right-hand side the true velocities are eliminated due to (2.8). As a result we obtain (2.12a) or (2.12b). Relation (2.12c) follows from (2.12a) or (2.12b). Relation (2.12a) or (2.12b) means that the saturation can be replaced by the relative permeability ratio. This fact is of considerable importance, as the measurement of the relative permeability ratio is a simpler and more accurate quantity than that of saturation.

2.4. MONOVARIANCE OF THE THERMODYNAMIC SUB-SYSTEM

Another significant property of steady-state compositional flow follows from thermodynamic sub-system (2.11).

It is seen that this sub-system contains $(3N + 4)$ equations and $(3N + 5)$ thermodynamic variables: $\zeta^{(k)}$, $c_g^{(k)}$, $c_o^{(k)}$, ρ_g , ρ_o , P , P_o , s . This means that a single (arbitrary) variable is independent. In other words the system variance is equal to 1.

Let us designate $P \equiv P_g$ as the independent thermodynamic variable. Then the monovariance means that during a steady-state flow all other thermodynamic variables are functions of P :

$$\begin{aligned} \zeta^{(k)} &= \zeta^{(k)}(P), & c_i^{(k)} &= c_i^{(k)}(P), & \rho_i &= \rho_i(P), \\ P_o &= P_o(P), & s &= s(P); & i &= g, o; & k &= 1, \dots, N \end{aligned} \quad (2.13)$$

2.5. STEADY-STATE MODEL FOR RADIAL FLOW

Let us examine now the steady-state radial flow towards a well between two radii r_w and r_e in a cylindrical domain of thickness h . Let the total flow rate of both phases $q = 2\pi rh[V_g\phi(1 - s) + V_o\phi s]$ is known at radius r_w . For q it is easy to obtain the following link with P using (2.8) and (2.10):

$$q = 2\pi rhV\phi[(1 - s) + s] = 2\pi rhV\phi = \frac{2\pi hkk_{rg}}{(1 - s)\mu_g}r \frac{dP}{dr}$$

Then the radial flow problem can be written using (2.10) and (2.13) as:

$$\frac{\partial}{\partial r} \left(\frac{rk_{rg}(s(P))}{[1 - s(P)]\mu_g} \frac{\partial P}{\partial r} \right) = 0, \quad r_w < r < r_e$$

$$P|_{r=r_e} = P_e, \quad \left. \frac{k_{rg}}{(1 - s)\mu_g}r \frac{\partial P}{\partial r} \right|_{r=r_w} = \frac{q}{2\pi kh}$$

The first integration yields:

$$\frac{k_{rg}}{(1 - s)\mu_g}r \frac{\partial P}{\partial r} = \frac{q}{2\pi kh} = \text{const}, \quad \forall r$$

The final solution is then:

$$\int_P^{P_e} \frac{k_{rg}(\bar{P})}{[1 - s(\bar{P})]\mu_g} d\bar{P} = \frac{q}{2\pi kh} \ln\left(\frac{r_e}{r}\right)$$

or

$$q = \frac{2\pi kh}{\ln\left(\frac{r_e}{r}\right)} \int_P^{P_e} \frac{k_{rg}(\bar{P})}{(1 - s(\bar{P}))\mu_g} d\bar{P} \tag{2.14}$$

If $P = P_o$, the last relationship can be written in the equivalent form, using (12c):

$$q = \frac{2\pi kh}{\ln\left(\frac{r_e}{r}\right)} \int_P^{P_e} \left[\frac{k_{rg}(\bar{P})}{\mu_g} + \frac{k_{ro}(\bar{P})}{\mu_o} \right] d\bar{P} \tag{2.15}$$

The integral operator in (2.15) is called the ‘pseudopressure integral’.

Thus, hydrodynamic equation (2.15) or (2.14) completed by a separate thermodynamic sub-system (2.11) represents a simple exact model of compositional flow towards a well. The advantages of this models are obvious:(i) no necessity to

perform fine-grid hydrodynamic simulations; (ii) the thermodynamic calculation block is entirely separated from the hydrodynamic model.

2.6. OBSERVATIONS

We see that a steady-state compositional flow through porous medium is characterized by the following properties:

1. the total flowing composition of mixture is constant in space;
2. the real flow velocities of both phases are identical; no relative velocity exists;
3. the thermodynamic sub-system (2.11) is entirely independent on hydrodynamics;
4. the thermodynamic behavior of a multicomponent two-phase system during steady-state flow in porous medium is monovariant, which means that all the thermodynamic variables, depend on pressure only;
5. the relative permeability ratio is a universal function of pressure defined as (2.12a) whatever the porous medium; hence, taking in account the previous property, the relative permeability ratio can be also examined as a pure thermodynamic variable;
6. the hydrodynamic sub-system for a 1D radial flow has analytical solution (2.15) or (2.14), which is similar to the Dupuit formula with replacing the pressure by pseudopressure integrals.

3. Factors Affecting Gas-Condensate Relative Permeability

To calculate gas-condensate well performance using basic relation (2.15), it is necessary to compute the pseudopressure integrals. In turn, they include thermodynamic variables and relative permeabilities. The calculation of thermodynamic variables as functions of pressure is based on system (2.11) and does not present any problems. Indeed, system (2.11) describes a classical PVT experiment performed for a mixture at a constant total composition.

The more complex problem is to calculate relative permeabilities for gas-condensate systems, that remains still a rather open problem.

According to the recent results of various researchers, the gas-condensate relative permeabilities depend on various parameters, not only on the saturation. Among the basic parameters influencing the relative permeability behavior it is necessary to note:

- the hysteresis phenomena in the vicinity of wells;
- the capillary number;
- the high-rate flow of gas and inertia effects;
- the medium heterogeneity and scale effects.

In the present paper we suggest a generalized model, which takes into account all of these effects.

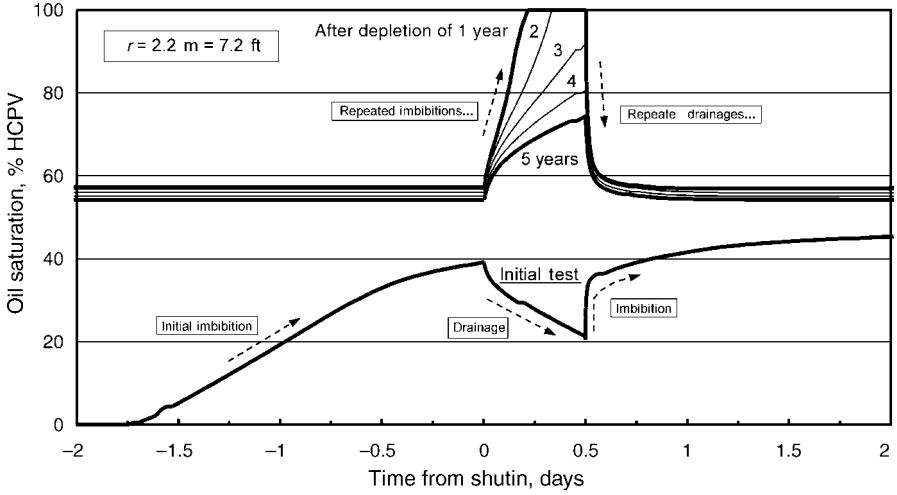


Figure 1. Saturation hysteresis prior-to and following the annual 12-hour shutins in a gas condensate well – at a radius of 2.2 m from the wellbore. Shows complete and partial cycles of drainage and imbibition.

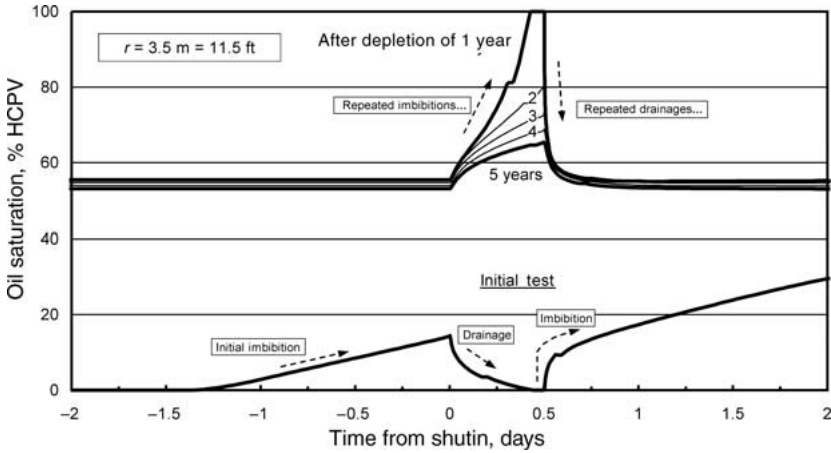


Figure 2. Same as Figure 1 but at a radius 2.2 m from the wellbore.

3.1. SATURATION HYSTERESIS IN THE VICINITY OF A WELL

We have found that the changing saturation history in the near-well region of a gas-condensate well is complex, as illustrated in Figures 1–4. The results were generated with a fine-grid radial EOS-based compositional model.

Repeated cycles of imbibition and drainage follow rate variations and shutin periods. Figures 1 and 2 show the saturation history of a well at radii of 2.2 and 3.5 m, where annual 12-hour shutins are imposed over a five-year period during depletion. Cycles of imbibition and drainage are repeated in association with each

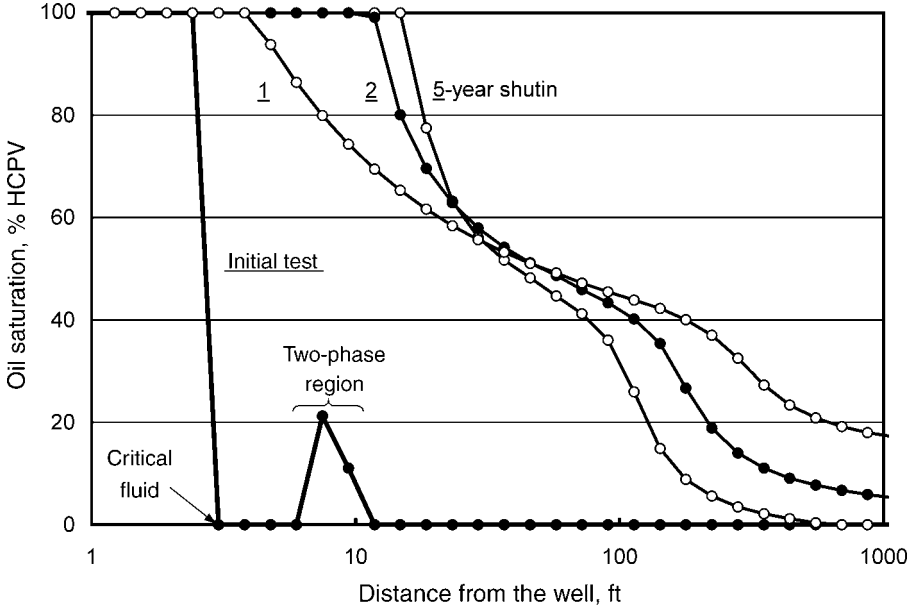


Figure 3. Saturation profiles following a 12-hour shutin for a gas condensate well – for a gas condensate well during the first five years of depletion. Shows the development of a solid oil ‘bank’ in the near-well region, as well as complex near-critical and two-phase regions beyond the oil bank.

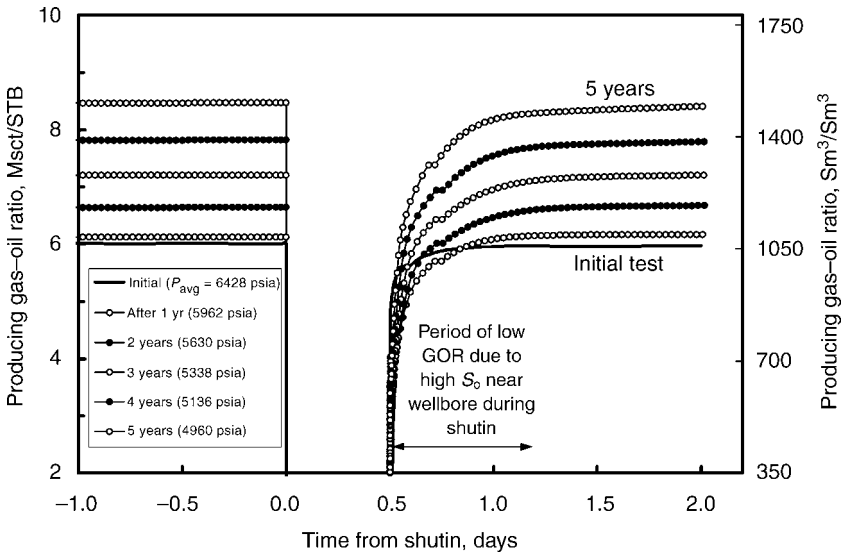


Figure 4. Producing GOR variation prior and following the annual 12-hour shutins – for a gas condensate well during the first five years of depletion. Post-shut-in GOR behavior shows overly-rich produced wellstream due the ‘emptying’ of the oil bank that develops near the well during the shut-in period.

shutin. Similar cycles of hysteresis (not shown) also follow changes in production rate, and particularly abrupt reductions in rate.

Figure 3 illustrates the complexity of saturation distribution around a well at the end of shutin periods. For the initial-test shutin, the *oil saturation* buildups up from a pre-shutin value of 20–40% to S_o values at the end of the shutin of (a) 100% at $r < 2$ ft, (b) a critical fluid at 2 ft (0 or 100%), (c) 0–20% in the small interval $r = 8$ –10 ft, and (d) 0% beyond 10 ft.

For subsequent shutins at 1, 2, and 5 years into depletion, the near-well region oil saturation increases from pre-shutin flowing saturations of about 55%, to end-shutin saturations of 100% near the well (3–20 ft), then monotonically decreases at increasing radii until the ‘average reservoir saturation’ (due to retrograde condensation) is approached far into the reservoir.

Production following the shutin will cause a significant drainage of the built-up near-well saturations as shown in Figures 1 and 2. This drainage behavior following shutins will be experienced with varying degree throughout the entire ‘condensate blockage’ zone. This *drainage process* will continue indefinitely (at any given point in the blockage zone) until a new BHFP increase is imposed by rate reduction or shutin.

The near-well saturation hysteresis varies from reservoir to reservoir, but similar cycles of large saturation change are common to *all* gas condensates during the life of a well. We consider this behavior to constitute severe hysteresis, but hysteresis that can not readily be modeled. The hysteresis is neither strictly ‘imbibition’ or strictly ‘drainage’ – but a complex series of drainage–imbibition cycles. *The most important issue is whether the effect of such hysteresis has a large or small impact on k_{rg} .*

3.2. REASONS OF SATURATION HYSTERESIS

Considerable misunderstanding can be found in the literature regarding relative permeabilities in gas condensate wells, and particularly with respect to whether the process is ‘imbibition’ or ‘drainage’. Let us remember that, according to definition, imbibition is a process of condensate saturation growth. In the theory of water–oil flow, the imbibition and drainage relative permeability curves are different and form a hysteretic loop.

It has been argued by Raghavan and Jones (1996) for gas-condensate flow that imbibition is the dominating process regarding the development of liquid phase during depletion of a gas-condensate reservoir. They claim that only a small volume of the reservoir near the well is affected by the drainage process, and the time over which this occurs is relatively short.

In reality, *only* in the far-removed region of the reservoir where condensate is continuously accumulating and oil saturation is continuously increasing, imbibition dominates. As discussed earlier, however, the relative permeability behavior in this ‘accumulation’ region has only a second-order or negligible effect on well performance.

We have conducted detailed well simulations using a compositional model and multiple C_{7+} fractions, with flowing BHP as low as 250 psia, without ever having observed that oil saturation near the wellbore ‘vaporizes’ to a zero (or low) saturation where oil has zero mobility. In fact, steady-state flow theory proves that as long as the BHP is greater than the lower dewpoint of the produced wellstream, then the threshold oil saturation $S_{ro} > 0$ and $k_{rg}/k_{ro} < \infty$, according to (2.12a), which guarantees two-phase gas/oil flow with both gas and oil saturations greater than zero.

The drainage actually experienced in the near-well region of a gas condensate well is mainly due to the rate changes and shutin periods that cause complete and partial cycles of imbibition and drainage. Even for the over-simplified case of a well producing at a constant BHP at all times, the oil saturation at the wellbore will increase initially (‘imbibition’), reach a maximum, and then decrease (‘drainage’) during the remaining life of the well; the decrease in saturation is not due to revaporization, but because the flowing mixture (produced wellstream) is getting leaner.

As for the duration of drainage period in the vicinity of wells, it is not at all short. First of all, for the simple case of a well producing against a constant BHP, the initial oil saturation increase – ‘imbibition’ – is always followed by an *extended* period of oil saturation decrease – ‘drainage’. The drainage process is caused by the flowing mixture in the near-well region becoming leaner. The leaner mixtures must have increasing k_{rg}/k_{ro} values. For higher k_{rg}/k_{ro} values (at a given pressure), k_{rg} must be increasing. This implies a decreasing oil saturation, which is a drainage process. For this simplified case, it is the *drainage process* that describes the entire ‘blockage’ region throughout most of the life of the reservoir.

In reality, the rate changes and shutin periods associated with normal (erratic) production behavior of actual gas condensate wells will lead to a much more complex saturation history than described above.

In conclusion, in the near-well region where condensate blockage occurs, practically unlimited cycles of drainage and imbibition hysteresis occur during shutins, rate changes, and by the continuous depletion process. What one ‘calls’ the process of saturation change in a gas-condensate well is of no importance. The only issue is whether the cycles of saturation change have a quantitative impact on the relative permeability behavior [of $k_{rg} = f(k_{rg}/k_{ro})$], and if so, how they should be modeled.

4. Relative Permeability Model for Gas-Condensate Systems

The key behavior of relative permeabilities for describing near-well flow of gas condensates and condensate ‘blockage’ as presented herein, include:

- relative permeability in the near-well region is the function of ratio k_{rg}/k_{ro} , instead of S ;
- we consider relative permeability as a function of capillary number and suggest the form of this function;

- for a high-velocity flow we suggest the so-called ‘effective relative permeability’ dependent now on flow velocity;
- for a heterogeneous reservoir at the macroscale we suggest a procedure of scaling for relative gas-condensate permeabilities.

4.1. RELATIVE PERMEABILITY DEPENDENT ON CAPILLARY NUMBER

If the capillary forces tend to zero, the mixture behaves as miscible. In this case the relative permeabilities will be converted to diagonals. In contrast, at very high capillary forces, the relative permeability tends to an invariable function typical for absolutely immiscible systems. All the intermediate curves will be obviously situated between these two limit functions.

We thus propose a generalized relative permeability model, where the ‘immiscible’ or ‘rock’ curves are linked with ‘miscible’ or ‘straight-line’ curves through a transition function dependent on capillary number, $f_1(N_c)$. The transition function is a smooth and continuous relation without a ‘threshold’ N_c value.

For low capillary numbers, the immiscible curves apply and $f_1 = 1$. For sufficiently high capillary numbers the miscible curves apply and $f_1 = 0$. A constant k_{rg}/k_{ro} value (used instead of saturation) defines the immiscible and miscible relative permeability values used in the generalized correlation.

The immiscible relative permeability models contain a number of (2–10) adjustable parameters, while the transition function f_1 has only two adjustable parameters. Non-linear regression locates the minimum (weighted sum-of-squares) deviation between measured and model k_{rg} data for a given set of measurements with varying k_{rg}/k_{ro} and N_c values.

Capillary number is defined as the ratio of viscous forces to capillary retaining forces

$$N_c = \frac{\Delta P_v}{P_c} \quad (4.1)$$

or, which is the same:

$$N_c = N_{cg} \equiv \frac{V_{pg} \cdot \mu_g}{\sigma_{go}}, \quad V_{pg} = \frac{V_g}{\phi \cdot (1 - S_{wi})} \quad (4.2)$$

where V_{pg} is a ‘pore’ gas velocity and V_g is Darcy’s gas velocity.

Relative permeability of gas including capillary number dependence is given by Whitson and Fevang (1997)

$$k_{rg} = f_1 \cdot k_{rgI} + (1 - f_1) \cdot k_{rgM} \quad (4.3)$$

where k_{rgI} is the immiscible ($N_c = 0$, $f_1 = 1$) gas relative permeability, and k_{rgM} is the miscible ($N_c = \infty$, $f_1 = 0$) straight line gas relative permeability, calculated as

$$k_{rgM} = k_{rg}^o \cdot \frac{1}{1 + (k_{rg}/k_{ro})^{-1}} \quad (4.4)$$

Our application of Equation (4.3) is different from others (Coats, 1980; Blom, 1999; Blom and Hagoort, 2003b) because we evaluate k_{rgI} and k_{rgM} at the same value of k_{rg}/k_{ro} – not at the same saturation. The limit to our approach is that it only can be used for the steady-state region where both gas and oil are flowing. The advantage is that only one set of parameters are required for correlating f_1 data, not four potentially separate sets for k_{rg} , k_{ro} , S_{gc} , and S_{oc} .

The transition function f_1 can be defined in the following way:

$$f_1 = \frac{1}{(\alpha \cdot N_c)^n + 1} \quad (4.5)$$

where α is a constant dependent only on rock properties. Based on regression of Heriot-Watt (Henderson *et al.*, 1995a, b) and Delft (Blom, 1999; Blom and Hagoort, 2003a) $k_{rg} = f(k_{rg}/k_{ro})$ data, we found a good estimate for α given by

$$\alpha = \frac{2 \cdot 10^4}{\sqrt{k\phi}}, \quad n = 0.7 \quad (4.6)$$

where K is absolute permeability and ϕ is porosity.

If saturation is used to link k_{rgI} to k_{rgM} and k_{roI} to k_{roM} , then separate parameters (n_g, α_g) and (n_o, α_o) are apparently needed for each phase. Experimental evidence by Blom (1999) suggest that $n_g < n_o$, $n_g \approx 1$ and $n_o \approx 1-3$ using saturation to link k_{rI} and k_{rM} ; also, $\alpha_g/\alpha_o = 1-100$.

Furthermore, with saturation as the ‘linking’ variable, critical saturations S_{oc} and S_{gc} must also be correlated from immiscible to miscible values using additional sets of parameters ($n_{S_{gc}}, \alpha_{S_{gc}}$) and ($n_{S_{oc}}, \alpha_{S_{oc}}$).

Clearly, the price for a more general treatment of capillary number dependence is additional complexity. Our experience is that the complexity is neither necessary or justified to match steady state gas–oil relative permeabilities needed in well calculations modeled with the pseudopressure approach. For cell-to-cell calculations in a model (e.g. a fine-grid radial model), the relative permeability model must be expressed in terms of saturation and our approach is no longer useful.

4.2. IMMISCIBLE RELATIVE PERMEABILITY MODELS

We have found three relative permeability correlations useful for describing low-capillary number ‘immiscible’ behavior of steady-state data measured for gas condensate cores.

The Corey model (Brooks and Corey, 1966; Standing, 1975):

$$\begin{aligned} k_{rg} &= k_{rg}^o \left[\frac{(1 - S_{oc})(1 - S_{wi}) + S_m - 1}{S_m - S_{wi}} \right]^2 \left[1 - S_{oc}^{\left(\frac{\lambda+2}{\lambda}\right)} \right], \\ k_{ro} &= k_{ro}^o \left[\frac{S_{oc} \cdot (1 - S_{wi}) - S_{oc}}{1 - S_{wi} - S_{oc}} \right] \cdot S_{oc}^{\left(\frac{\lambda+2}{\lambda}\right)} \end{aligned} \quad (4.7)$$

where $S_{oc} \equiv \frac{S_o}{1 - S_{wi}}$.

The Chierici model (Chierici, 1984):

$$k_{rg} = k_{rg}^o \cdot \exp(-B \cdot R_g^{-M}), \quad k_{ro} = k_{ro}^o \cdot \exp(-A \cdot R_o^L) \tag{4.8}$$

where

$$R_g = \frac{S_g - S_{gc}}{1 - S_{wi} - S_g} (S_g > S_{gc}), \quad R_o = \frac{S_g}{1 - S_{wi} - S_{oc} - S_g}$$

The Arco model (Jerauld, 1997):

$$\begin{aligned} k_{rg} &= k_{rg}^o (1 + c_{g2}) \cdot S_{ge}^{c_{g1}} \cdot (1 + c_{g2} \cdot S_{ge}^{c_{g3}})^{-1}, \\ k_{ro} &= k_{ro}^o (1 + c_{o2}) \cdot S_{oe}^{c_{o1}} \cdot (1 + c_{o2} \cdot S_{oe}^{c_{o3}})^{-1} \\ c_{g3} &= c_{g1} \cdot \left(1 + \frac{1}{c_{g2}}\right), \quad S_{ge} \equiv \frac{S_g - S_{gc}}{1 - S_{wi} - S_{gc}}, \\ c_{o3} &= c_{o1} \cdot \left(1 + \frac{1}{c_{o2}}\right), \quad S_{oe} \equiv \frac{1 - S_g - S_{wi} - S_{oc}}{1 - S_{wi} - S_{oc}} \end{aligned} \tag{4.9}$$

Using relation (12a) between saturation and relative permeability ratio, it is easy reconstruct all these functions in the form of $k_{rg} = f(k_{rg}/k_{ro})$, $k_{ro} = f(k_{rg}/k_{ro})$.

We generally use one of these three correlations to fit data in the form $k_{rg} = f(k_{rg}/k_{ro})$ – that is, without the need for measured saturations. It is important to realize that the three correlations can usually describe similar $k_{rg} = f(k_{rg}/k_{ro})$ behavior but with somewhat different $k_r(S)$ behavior. This is illustrated in Figures 5–7.

Figure 5 shows the more-or-less same $k_{rg} = f(k_{rg}/k_{ro})$ behavior for the entire range of k_{rg}/k_{ro} of interest to gas condensate wells (0.1–100). Figure 6 shows the $k_r(S)$ curves on a semi-log plot, enclosing with a box the area of interest where k_{rg}/k_{ro} ranges from 0.1 to 100.

Figure 7 shows the $k_r(S)$ curves on a cartesian plot, enclosing with a box the area of interest (to some rich gas condensates) where $k_{rg}(S)$ may have a second-order effect on pressure loss calculations in the ‘accumulation’ region away from the well (Region 2 in the Fevang–Whitson paper (Fevang and Whitson, 1996)). If saturation measurements are made, they should be made in this region. These S_o data, if available, can be used together with the $k_{rg} = f(k_{rg}/k_{ro})$ data in fitting the relative permeability correlation.

4.3. RELATIVE PERMEABILITY SCALING IN HETEROGENEOUS STRATA

The different rock types in a full-field simulation model must be assigned consistent relative permeability data. The best modeling approach is to develop a relative permeability correlation that is general for all rock types, or to develop separate correlations for each rock type that exhibits considerably different relative permeability behavior [$k_{rg} = f(k_{rg}/k_{ro})$ behavior]. However, this approach requires a

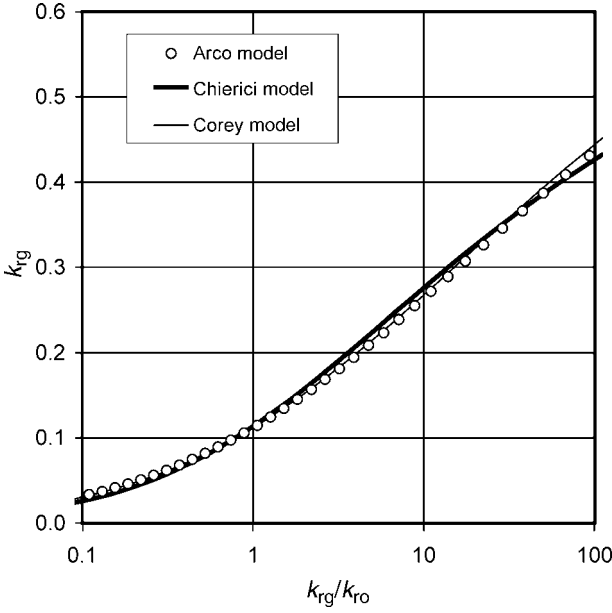


Figure 5. Fundamental $k_{rg} = f(k_{rg}/k_{ro})$ relationship using three different immiscible correlations, showing essentially identical behavior in the entire range of k_{rg}/k_{ro} of interest (from very rich to very lean gas condensate systems).

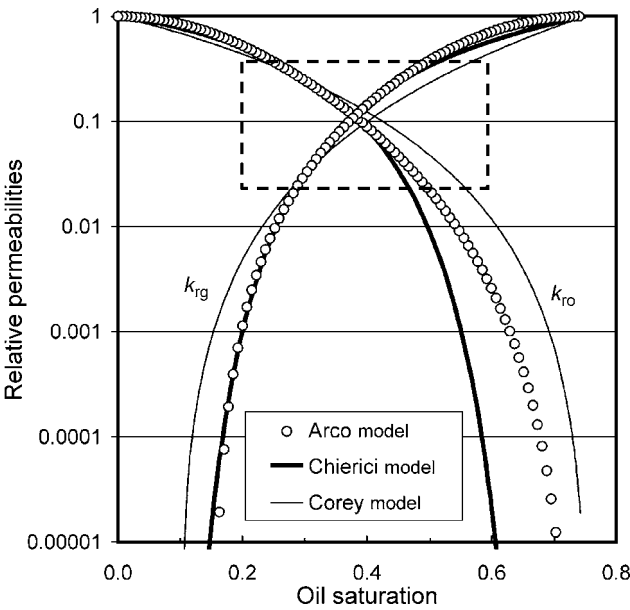


Figure 6. Saturation dependent relative permeability curves for three correlations, showing in particular the region that affect flow behavior in the near-well region (boxed area). The three correlations have the ‘same’ $k_{rg} = f(k_{rg}/k_{ro})$ relationship in the boxed region.

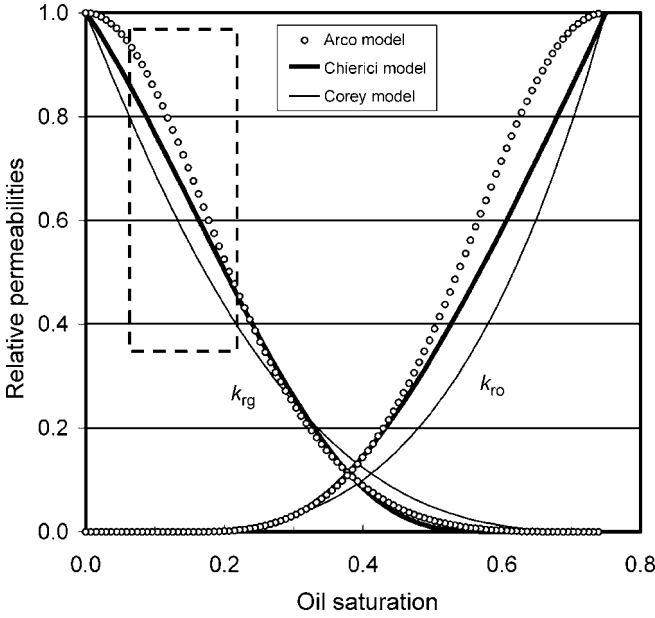


Figure 7. Saturation dependent relative permeability relations for three correlations, showing in particular the region that affect flow behavior in the ‘distant’ accumulation region away from the well (boxed area). The three correlations have the ‘same’ $k_{rg} = f(k_{rg}/k_{ro})$ relationship.

large number of measured data (for each rock type) – data which are usually not available.

When only *limited* relative permeability data are available, end-point scaling can be used to generate relative permeability for different rock types. Our procedure for endpoint scaling of relative permeability uses the *same* scaling for both gas (k_{rg}) and oil relative permeability (to gas, $k_{ro,g}$) curves. For a reference set of relative permeability curves,

$$k_{rg}^{ref} = f(S_g^{ref}, S_{wi}^{ref}, S_{gc}^{ref}, S_{oc}^{ref}), \quad k_{ro}^{ref} = f(S_g^{ref}, S_{wi}^{ref}, S_{gc}^{ref}, S_{oc}^{ref})$$

$$S_g = S_{gc} \frac{S_g^{ref}}{S_{gc}^{ref}}, \quad S_g \leq S_{gc}$$

$$S_g = S_{gc} + \frac{(1 - S_{wi} - S_{oc} - S_{gc})}{(1 - S_{wi}^{ref} - S_{oc}^{ref} - S_{gc}^{ref})} (S_g^{ref} - S_{gc}^{ref}),$$

$$S_{gc} < S_g \leq 1 - S_{wi} - S_{oc}$$

$$S_g = 1 + S_{wi} + S_{oc} + \frac{S_{oc}}{S_{oc}^{ref}} (S_g^{ref} - 1 - S_{wi}^{ref} - S_{oc}^{ref}),$$

$$1 - S_{wi} - S_{oc} < S_g \leq 1 - S_{wi}$$

$$S_g = 1 - S_{wi} + \frac{S_{wi}}{S_{wi}^{ref}} (S_g^{ref} - 1 + S_{wi}^{ref}), \quad 1 - S_{wi} < S_g \leq 1$$

The relative permeabilities are scaled with the ratio:

$$k_{rg}(S_g) = k_{rg}^{ref}(S_g^{ref}) \cdot k_{rg}(S_{wi}) / k_{rg}(S_{wi}^{ref}),$$

$$k_{ro}(S_g) = k_{ro}^{ref}(S_g^{ref}) \cdot k_{ro}(S_{wi}) / k_{ro}(S_{wi}^{ref})$$

This endpoint scaling procedure ensures a reasonable $k_{rg}(k_{rg}/k_{ro})$ relationship for a wide range of endpoints. We have even found that the procedure is a good approximation for reservoirs when sufficient data is available to develop independent correlations for each rock type.

4.4. RELATIVE PERMEABILITY MODEL FOR HIGH-VELOCITY INERTIAL FLOW

To quantify the effect of inertial HVF pressure loss, an ‘effective’ gas relative permeability k_{rgHVF} is defined. The HVF is usually described by the so-called Forchheimer equation:

$$-\frac{\partial P}{\partial x} = \frac{\mu}{k} V + \beta \rho V^2$$

Let us rewrite this equation in the form of Darcy’s law:

$$-\frac{\partial P}{\partial x} = \frac{\mu}{k_{HVF}} V$$

where k_{HVF} is the effective absolute permeability, which depend now on flow velocity V .

In the same way the effective relative gas permeability, k_{rgHVF} , may be defined as that function make equivalent the formal two-phase Darcy equation to the two-phase Forchheimer equation. Starting with a single-phase relation for the inertial HVF coefficient β ,

$$\beta = ak^b \phi^c$$

it should be noted that various references give a wide range in constants: $a \sim 10^9-10^{10}$, $b \sim 0.5-1.5$, and $c \sim 0-5.5$. A number of authors have also treated the correction of β for relative permeability effect (see Blom and Hagoort (2003b) for a review), where we use the relation

$$\beta_{eff} = \beta \cdot k_{rg}^{-b'} \tag{4.10}$$

with $b' = b$. The choice of correlation for β can have a profound affect on the magnitude of inertial HVF and the effect of relative permeability on β_{eff} . In the examples presented below, we use $a = 9 \cdot 10^9$, $b = b' = 1$, and $c = 0.75$.

Our suggestion is to use an effective gas relative permeability corrected for high velocity effect k_{rgHVF} , defined as

$$\frac{k_{rgHVF}}{k_{rg}} = \left[1 + \frac{k \cdot k_{rg}}{\mu_g} \cdot \beta_{eff} \cdot \rho_g \cdot V_g \right]^{-1} \tag{4.11}$$

Effective oil relative permeability including the effect of HVF is calculated by dividing k_{rgHVF} by k_{rg}/k_{ro} .

4.5. VELOCITY DEPENDENCE IN PSEUDOPRESSURE

Relationships (4.2) for capillary number and (4.11) for the effective HVF relative permeability include the flow velocity V . It is necessary to find a relation that gives velocity as a function of pressure so that capillary number and inertial HVF effects can be included in the pseudopressure function (2.15) through relative permeability. Our approach is outlined here for radial flow, with similar equations used for linear flow in vertically-fractured wells.

A trivial relation exists between the flow rate and the velocity: $V = qB/2\pi hr$. Inverting this equation with respect to the radius, we obtain:

$$r = \frac{qB}{2\pi hV} \quad (4.12)$$

Let us insert now this relation into (2.15), eliminating thus variable r :

$$q = \frac{2\pi h}{\mu B \ln\left(\frac{r}{r_w}\right)} (P_p - P_{pwf})$$

where $\Phi(P)$ is the pseudopressure integral.

Then we obtain for the velocity as the function of pressure:

$$V(p) = \frac{qB}{2\pi hr_w} \exp\left[-\frac{2\pi kH}{q\mu B} (P_p - P_{pwf})\right] \quad (4.13)$$

Knowing velocity V as a function of pressure, capillary number is also given in terms of pressure, and the pseudopressure function can be evaluated including capillary number dependence of relative permeabilities. Knowing k_{rg} , the correction to include inertial HVF can be calculated using Equation (4.11), where k_{rgHVF} should then be used in the final pseudopressure calculation.

The equations above can readily be extended to linear flow for vertically-fractured wells.

An example is presented using the pseudopressure method for calculating reservoir well performance of a rich gas condensate with two well configurations (radial and vertically-fractured). Figures 8–13 present results of the calculations.

Figures 8 and 9 show the rate–time performance for three assumptions: (a) no N_c dependence on $k_{rg} = f(k_{rg}/k_{ro})$, (b) N_c dependence included using our proposed correlation, Equation (4.3), and (c) both N_c dependence and inertial HVF effects included. For this example, the capillary number dependence has a significant impact on rate–time predictions, while the inertial HVF effect has only a second-order effect.

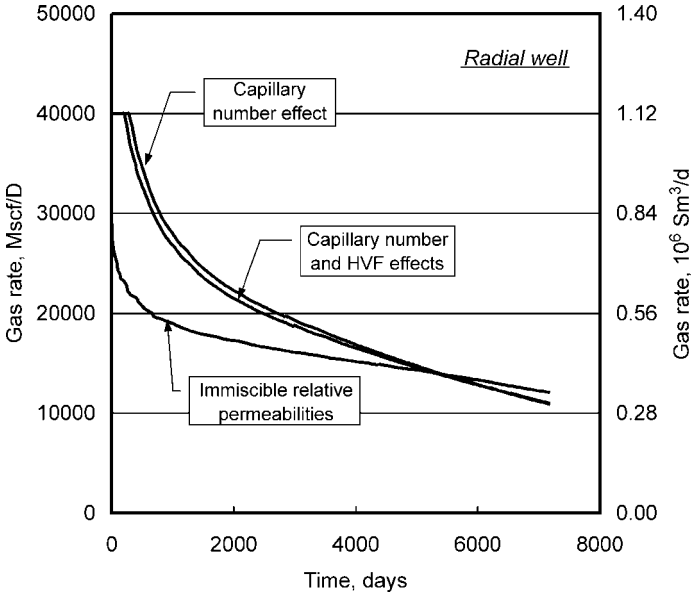


Figure 8. Rate-time behavior for a rich gas condensate radial well showing the effect of including capillary number improvement of k_{rg} , and inertial high velocity flow ('turbulence').

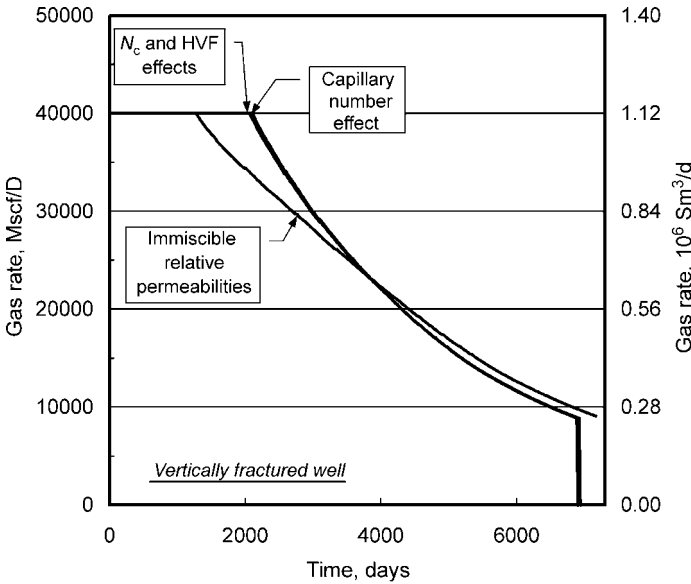


Figure 9. Rate-time behavior for a rich gas condensate vertically-fractured well showing the effect of including capillary number improvement of k_{rg} , and inertial high velocity flow ('turbulence').

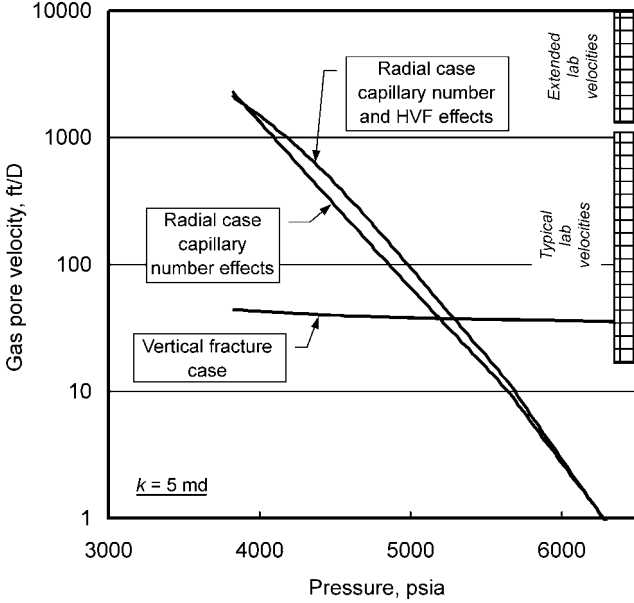


Figure 10. Example gas ‘pore’ velocities variation with pressure for radial and vertically-fractured (linear) flow geometries in a rich gas condensate well using proposed steady-state pseudopressure model.

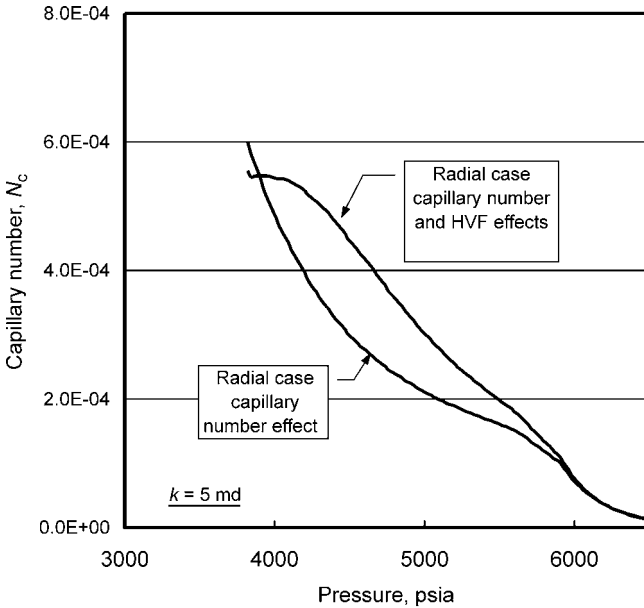


Figure 11. Example capillary number variation with pressure for radial flow geometry in a rich gas condensate well using proposed steady-state pseudopressure model; also shows effect of inertial HVF (‘turbulence’) on capillary number.

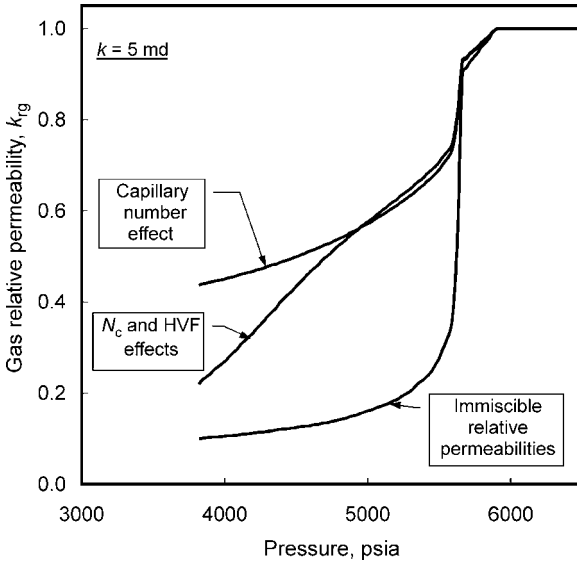


Figure 12. Example of gas relative permeability variation with pressure for radial flow geometry in a rich gas condensate well using proposed steady-state pseudopressure model; shows effect of N_c dependence on k_{rg} and effect of inertial HVF ('turbulence') on capillary number.

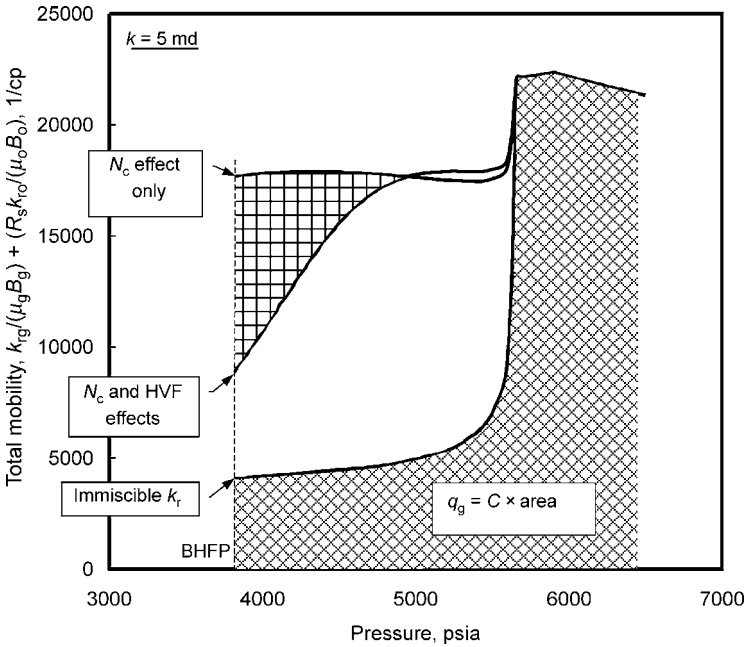


Figure 13. Example total mobility (pseudopressure function) variation with pressure for radial flow geometry in a rich gas condensate well using proposed steady-state pseudopressure model; shows effect of N_c dependence on k_{rg} and inertial HVF ('turbulence') on capillary number.

Looking at the radial well calculations in more detail, Figures 10–13 show the pressure dependence of gas pore velocity, capillary number, gas relative permeability, and total mobility. These figures show quantitatively how the capillary number and inertial HVF affect relative permeability and total mobility. It seems clear that the capillary number dependence can be an important factor in predicting reservoir well performance (i.e. condensate blockage) and, consequently, should be measured in the laboratory and correlated for model calculations.

Though the effect of inertial HVF was not particularly important in this example we have found a number of field case histories where inertial HVF in a vertical fracture (or in perforations; Stewart, 1997) has had a major impact on the well deliverability. Considerable uncertainty in prediction of β and its dependence on relative permeability exists with today's correlations – more than one order of magnitude. Consequently we recommend that additional measurements be made to improve our quantitative prediction of inertial HVF in gas condensate systems.

5. Experimental Measurement of Gas-Condensate Relative Permeabilities

Our recommendation for measuring relative permeability data used in well modeling of gas condensate reservoirs is outlined below.

5.1. DEFINING THE RANGE OF RELEVANT k_{rg}/k_{ro} DATA

Using Equation (2.12a), it is easy to evaluate the general range of k_{rg}/k_{ro} variation in a gas-condensate reservoir. When applied to the near-well region, saturation $s = v_{ro}$ in (2.12a) is then the ratio of oil volume to total gas + oil volume of the mixture flowing into a well (produced wellstream), evaluated at pressures existing in the near-wellbore region. For example, a 'rich' gas condensate at relatively moderate flowing near-wellbore pressures (100–200 bar) $s = v_{ro}$ may be about 0.2. The μ_g/μ_o ratio is typically about 0.025/0.1 or about 0.25. This leads to a $k_{rg}/k_{ro} = (1/0.2-1)(0.25) = 1$ [the crossing point of the relative permeability curves]. As the reservoir depletes, the flowing wellstream becomes leaner and $s = v_{ro}$ will decrease to a lower value – for example, $S=0.025$. Interestingly, near-wellbore viscosities are more-or-less constant during depletion and the resulting late-life $k_{rg}/k_{ro} = (1/0.025-1)(0.25) = 10$.

This simple example illustrates the observation that the range of k_{rg}/k_{ro} experienced by a gas condensate well during its entire life of depletion will vary by only about one order of magnitude. The k_{rg} variation is even smaller – perhaps from 0.05 to 0.2 in this 'rich' condensate example. Consequently, our approach to measuring relative permeabilities is to (1) determine the expected range of k_{rg}/k_{ro} spanned for a given reservoir from PVT properties of the gas condensate fluid system, then (2) concentrate on obtaining accurate k_{rg} data in this range of

k_{rg}/k_{ro} . The measurements are preferably made at realistic flowing pressures and velocities.

We recommend that, as a minimum, five *immiscible* k_{rg} data be measured for a specific range of k_{rg}/k_{ro} values. These k_{rg}/k_{ro} values are those which dominate flow in the condensate blockage region near the well, and they are defined *only by PVT properties* of the fluid system (Equation (2.12a)).

First, a constant-volume depletion (CVD) experiment is simulated. For each CVD gas removed, a constant-composition experiment (CCE) is simulated, reporting $s = v_{ro} = V_o/V_t$ and the viscosity ratio μ_g/μ_o for pressures from the gas dewpoint (CVD pressure) down to a ‘minimum’ pressure. These PVT quantities are used in Equation (2.12a) to calculate $k_{rg}/k_{ro}(p)$.

The CVD pressures should cover the range from initial dewpoint to the expected abandonment reservoir pressure. The minimum CCE pressure should be selected to represent the lowest BHFP expected (when the well is on decline).

Figure 14 shows an example plot of $k_{rg}/k_{ro}(p)$. The range of ‘relevant’ k_{rg}/k_{ro} is more-or-less given by the k_{rg}/k_{ro} values near the minimum BHFP (marked with closed circles). For this lean gas condensate, the range of k_{rg}/k_{ro} is from about 5 to 50 during the entire life of the well. Typically the relevant range of k_{rg}/k_{ro} is about 1 to 1-1/2 cycles (e.g. 0.5–10 for a rich condensate and 10–100 for a very lean condensate).

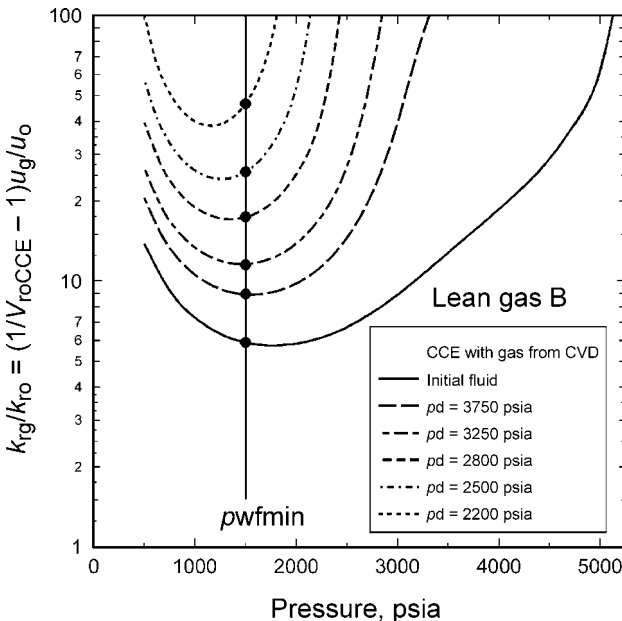


Figure 14. Design plot for determining the relevant range of k_{rg}/k_{ro} during depletion of a gas condensate reservoir, where the k_{rg}/k_{ro} values of interest are close to the minimum BHFP.

5.2. IMMISCIBLE STEADY-STATE MEASUREMENTS

Each *immiscible* k_{rg} data should be measured by flowing a pre-selected reservoir gas (with known k_{rg}/k_{ro}) under steady-state conditions at a core pressure close to the minimum BHFP. When steady-state is achieved the pressure drop is measured, and k_{rg} is calculated from the gas flow rate, pressure drop, and gas viscosity; k_{ro} is calculated from $k_{ro} = k_{rg}/(k_{rg}/k_{ro})$.

Steady-state flow can be achieved either by flowing the reservoir (CVD) gas through a back-pressure regulator upstream to the core, thereby lowering the pressure to a value close to the minimum BHFP; else it can be measured by equilibrating the reservoir gas at core pressure and injecting the equilibrium gas and oil at rates that ensure the correct k_{rg}/k_{ro} value given by Equation (2.12a) [noting $q_o/(q_g + q_o) = V_{ro}(p_{core})$].

The five immiscible data should be selected using five flowing mixtures (e.g. CVD gases) that provide more-or-less evenly-spaced k_{rg}/k_{ro} values in the range of interest.

5.3. HIGH CAPILLARY NUMBER MEASUREMENTS

Based on the maximum expected (plateau) rates for a given field using the initial reservoir fluid, the flow velocities can be estimated at the minimum BHFP. At these conditions, a capillary number can be calculated. This capillary number can be used in our correlation for f_1 , Equations (4.5) giving the expected improvement in k_{rg} from Equation (4.3).

As an example, consider a field with $q_{gmax} = 2 \cdot 10^6 \text{ Sm}^3/\text{d}$, $h = 100 \text{ m}$, $r = 1 \text{ m}$, $\phi = 0.2$, $S_w = 0.25$, $B_{gd}(100 \text{ bar}) = 0.0125$, $\mu_g = 0.02 \text{ mPa s}$, $V_{pg} = 0.03 \text{ m/s}$ [$V_{pg} = q_{gmax} B_{gd}(p_{wf}) / (2\pi r h \phi (1 - S_w))$]. With a gas-oil IFT of $\sigma_{go} = 3 \text{ mN/m}$ at 100 bar, $N_c = V_{pg} \mu_g / \sigma_{go} = 2 \cdot 10^{-4}$. For a permeability of $k = 50 \text{ md}$, Eq. (22). Equation (4.5) $\alpha = 2 \cdot 10^4 / [(50)(0.2)]^{0.5} = 7320$. The immiscibility factor f_1 at these conditions is $f_1 = 1 / (1 + [(7320)(2 \cdot 10^{-4})]^{0.7}) = 0.434$, which is a significant improvement in $k_{rg} = 0.434(0.1) + (1 - 0.434)(0.5) = 0.33$ (compared with $k_{rgI} = 0.1$).

Steady-state measurements (at minimum BHFP) can be made at high flow velocities in the laboratory to achieve higher capillary numbers. However, this has two disadvantages: (1) maximum laboratory pump rates do not usually allow reaching N_c values close to field values, and (2) even if field velocities could be reached, the effect of 'inertial' HVF pressure drop may become significant and confuse the interpretation of k_{rg} measurements.

Alternatively, we suggest measuring steady-state flow at higher core pressures with lower gas-oil IFTs. Higher flow velocities can still be used to reach high (near-field) capillary numbers, but it should first be established (e.g. with single-phase gas flow tests) that inertial HVF effects do not occur at these velocities.

Value k_{rg} should be measured at several velocities for each flowing mixture, and measurements can be repeated at a number of core flowing pressures (i.e. IFT values). To accurately correlate the capillary number, a few IFT measurements may be necessary to tune the IFT correlation (parachors); this is particularly true if $\sigma_{og} < 0.1$ mN/m, where the parachor correlation can be rather inaccurate.

5.4. SELECTING A SYNTHETIC GAS MIXTURE

We have found that the same $k_{rg} = f(k_{rg}/k_{ro})$ relation exists for actual reservoir gas condensate and synthetic gas condensate selected to mimic the key PVT behavior of the actual reservoir fluid system. The selection of a synthetic gas can be chosen using pure hydrocarbon compounds (e.g. C_1 - C_8 - C_{16}), where the molar quantities of the synthetic mixture are determined (automatically by regression) to match the approximate dewpoint, V_{ro} , and Z -factor behavior of the reservoir gas. It is also helpful if the gas-oil viscosity ratio is reasonably close to the reservoir fluid system (at pressures below the dewpoint). Figure 15 shows two examples of synthetic gas V_{ro} behavior compared with reservoir fluid CCE liquid dropout curves.

There is some evidence (e.g. the data of Ham and Eilerts (1967)) that the steady-state $k_{rg} = f(k_{rg}/k_{ro})$ behavior is independent of the fluid system (see Figure 16).

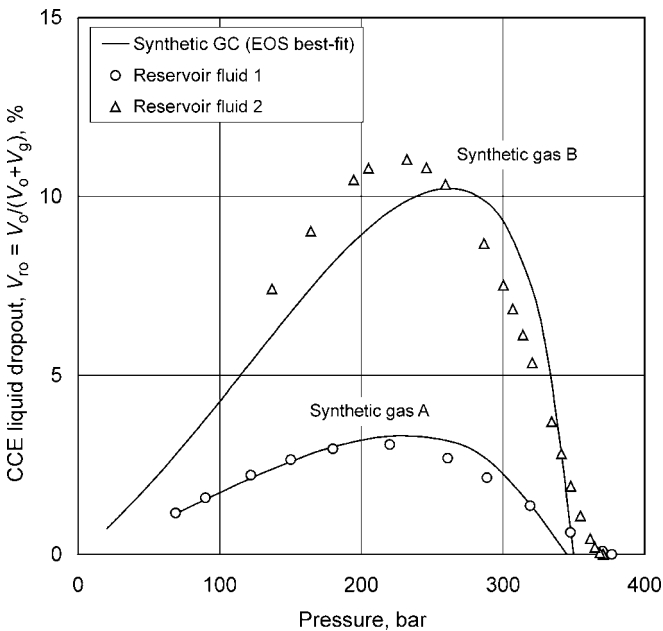


Figure 15. Example comparisons of oil relative volume behavior between two reservoir fluids and their synthetic gas ‘best-fit’ mixtures.

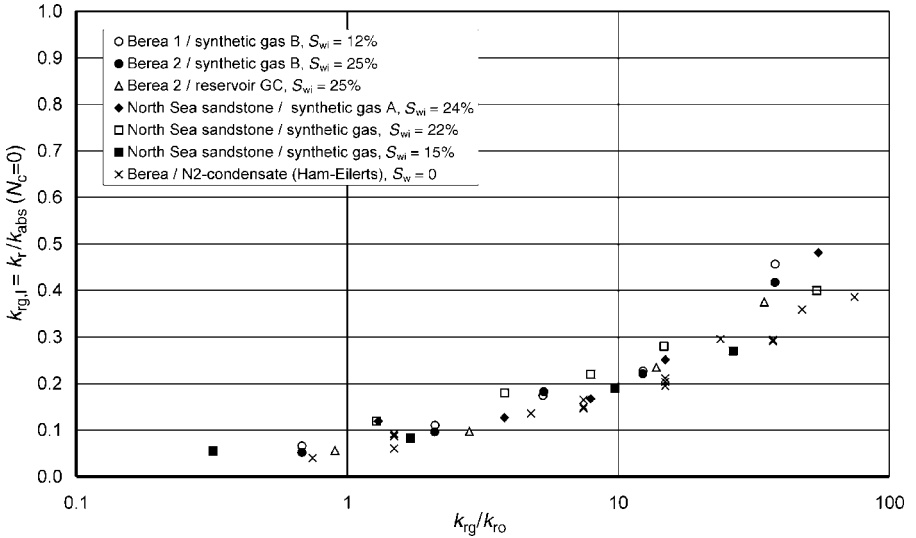


Figure 16. Immiscible (low- N_c) relative permeability measurements for two Berea and one North Sea sandstone compared with results for a Berea sample reported by Ham and Eilerts (1967).

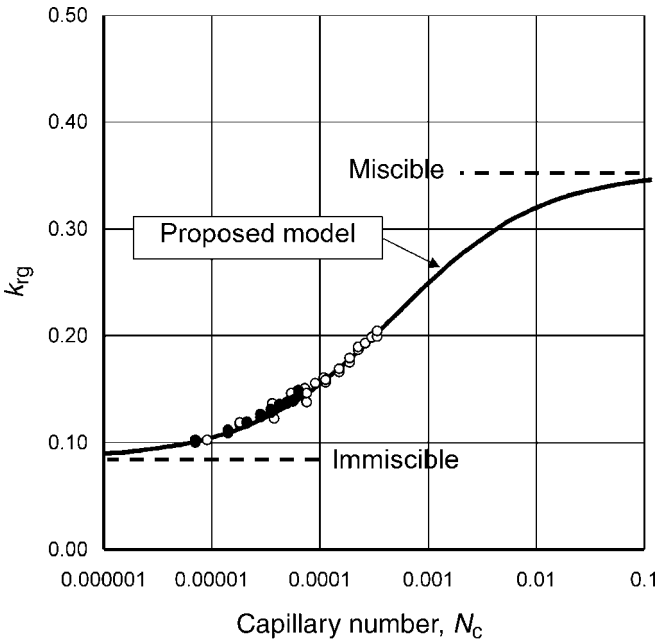


Figure 17. Fit of measured k_{rg} data with the proposed relative permeability model for a wide range of capillary numbers and a more-or-less constant $k_{rg}/k_{r0} = 2$.

Additional research is necessary to verify this supposition, but clearly it would make the measurement of *immiscible* k_{rgI} data much simpler. Still, to measure the capillary number dependence of the $k_{rg} = f(k_{rg}/k_{ro})$ relation, synthetic systems with low IFTs must be used.

5.5. FITTING RELATIVE PERMEABILITY DATA

Our procedure for fitting measured relative permeability data correlates $k_{rg} = f(k_{rg}/k_{ro}, N_c)$ using an immiscible equation for k_{rgI} (Arco, Corey, or Chiriaci), and the proposed correlation for capillary number dependence. Exponents and end-point saturations can be modified in the immiscible correlations, while the N_c correlation has only two adjustable parameters, α and n .

Figure 17 show an example fit of measured data for a Berea core and a medium-rich fluid system flowing with a $k_{rg}/k_{ro} = 2-3$ for a wide range of capillary numbers (velocities and core pressures). The closed circles are measurements using the reservoir gas condensate system, and the open circles are measurements using the ‘best-fit’ synthetic gas mixture. Gas–oil IFTs for the synthetic gas were in the range 0.8–1.6 mN/m, while for the reservoir gas the estimated IFT was 6.3 mN/m. The proposed correlation is shown as the solid line.

Figures 18 and 19 show the results of our proposed relative permeability model used to fit data measured by Marathon (Chen *et al.*, 1999) for a near-critical North Sea gas condensate. The open circles are low-pressure laboratory unsteady-state

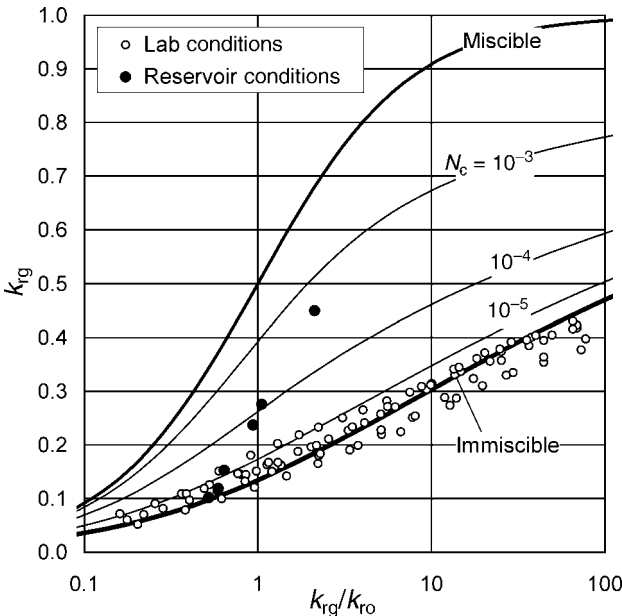


Figure 18. Fit of all available k_{rg} data using the proposed relative permeability model.

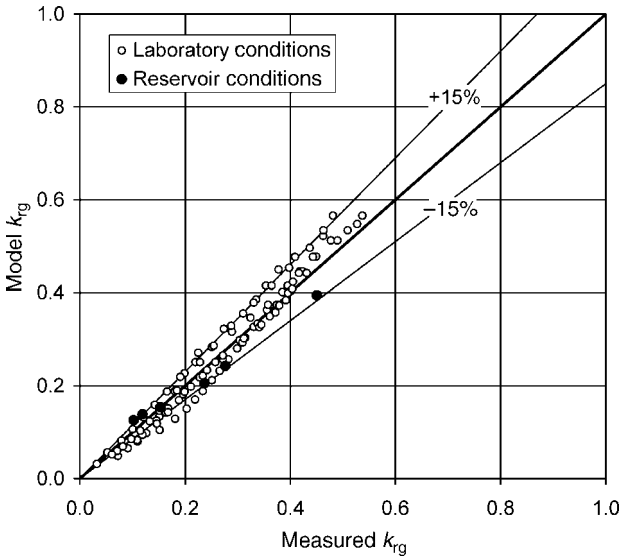


Figure 19. Quality of fit to measured relative permeability data from a North Sea rich gas condensate field using proposed model including capillary number dependence of $k_{rg} = f(k_{rg}/k_{ro})$.

measurements from seven different cores. The solid symbols are measured data using a stack of reservoir cores, flowing initial reservoir gas through the core-stack using a steady-state procedure at varying core pressures. The reservoir-condition data had varying gas–oil IFTs (0.026–0.54 mN/m) and capillary numbers ($2.2 \times 10^{-4} - 7.8 \times 10^{-6}$). The overall fit is shown in Figure 19, indicating that all data are correlated within about 15%.

If saturation data are available, they also can be used in the model parameter fit. However, the only situation we have found where saturation dependence of k_{rg} is important is when the oil saturation in Region 2 (accumulation region outside the condensate blockage zone) reaches values of 15–30%. This is only experienced by medium to rich gas condensates, and even then the effect is second order to the primary k_{rg} reduction in the near-well region.

Conclusions

1. The oil saturation history experienced in the near-well region of a gas condensate well consists of an unlimited number of cycles of complete or partial drainage and imbibition.
2. Based on our steady-state measurements (Saevareid *et al.*, 1999) of several gas condensate systems we have found that the effect of saturation hysteresis is small on the fundamental relative permeability relation $k_{rg} = f(k_{rg}/k_{ro})$.
3. A design procedure is proposed for defining the laboratory conditions and flowing mixtures that will ensure measurement of relative permeability beha-

vior at relevant flow conditions for the near-well region dictating condensate blockage.

4. The effect of capillary number on gas/oil relative permeability can result in a significant improvement in gas relative permeability and thereby reduce the negative impact of condensate blockage.
5. An empirical but consistent model is proposed for scaling gas/oil relative permeabilities for different rock types and regions with varying end-point saturations. The scaling is applied consistently to the gas and oil relative permeabilities to ensure that the reference (measured) $k_{rg} = f(k_{rg}/k_{ro})$ relation is honored.
6. An approach is given for incorporating (a) the improvement in k_{rg} at high capillary numbers, and (b) the detrimental effect of inertial high velocity flow ('turbulence') as part of the two-phase condensate pseudopressure model. The key to this approach is estimating velocity as a function of pressure in the reservoir using an appropriate form of Darcy's law for the well-flow geometry.

Acknowledgements

We thank the participants of the 'Gas Condensate Well Performance' project – BP, Chevron, INA, Mobil, Norsk Hydro, Norwegian Research Council (NFR), Norwegian Petroleum Directorate (NPD), Occidental International, and Saga Petroleum – for financial and technical support during the two years this work was conducted (1996–1998). We also thank Kameshwar Singh for his assistance. Finally, we acknowledge the theoretical development in section 2 to Prof Mikhail Panfilov.

References

- Al-Hussainy, R., Ramey, Jr., H. J. and Crawford, P. B.: 1966, The flow of real gases through porous media, *JPT*, 624; *Trans. AIME*, 237.
- Blom, S. M. P.: 1999, Relative permeability to near-miscible fluids, PhD Thesis, Delft University.
- Blom, S. M. P. and Hagoort, J.: 2003a, Relative permeability at near-critical conditions, Paper SPE 38935.
- Blom, S. M. P. and Hagoort, J.: 2003b, The combined effect of near-critical relative permeability and non-darcy flow on well impairment by condensate drop-out, Paper SPE 39976.
- Brooks, R. H. and Corey, A. T.: 1966, Properties of porous media affecting fluid flow, *J. Irrigation Drainage Division, Proc. of ASCE*, 92(No. IR2), 61–88.
- Chen, H. L., Wilson, S. D. and Monger-McClure, T. G.: 1999, Determination of relative permeability and recovery for North Sea gas-condensate reservoirs, *SPE*, 393–402.
- Chierici, G. L.: 1984, Novel relation for drainage and imbibition relative permeabilities, *SPEJ*, 275–276.
- Coats, K. H.: 1980, An equation of state compositional model, *SPEJ*, 363–376.
- Evinger, H. H. and Muskat, M.: 1942, Calculation of theoretical productivity factor, *Trans. AIME* 146, 126–139.
- Fevang, Ø. and Whitson, C. H.: 1996, Modeling gas-condensate well deliverability, *SPE*.
- Ham, J. D. and Eilerts, C. K.: 1967, Effect of saturation on mobility of low liquid–vapor ratio fluids, *SPEJ*, 11–19.

- Henderson, G. D., Danesh, A., Teherani, D. H., Al-Shaidi, S. and Peden, J. M.: 1995a, Measurement and correlation of gas condensate relative permeability by the steady-state method, *SPEJ* **1**(2), 191–201.
- Henderson, G. D., Danesh, A., Tehrani, D. and Peden, J. M.: 1995b, The effect of velocity and interfacial tension on the relative permeability of gas condensate fluids in the wellbore region, *8th European IOR Symposium*, May 15–17, 1995, Vienna.
- Janicek, J. D. and Katz, D. L.: 1955, Applications of unsteady state gas flow calculations, in reprint from the *U. Michigan Research Conference*, June 1955.
- Jerauld, G. R.: 1997, General three-phase relative permeability model for Prudoe Bay, *SPERE*, 255–263.
- Jones, J. R. and Raghavan, R.: 1985, Interpretation of flowing well response in gas condensate wells, Paper SPE 14204 presented at the *1985 SPE Annual Technical Conference and Exhibition*, Las Vegas, September 22–25.
- Jones, J. R., Vo, D. T. and Raghavan, R.: 1986, Interpretation of pressure buildup responses in gas condensate wells, Paper SPE 15535 presented at the *1986 SPE Annual Technical Conference and Exhibition*, New Orleans, October 5–8.
- Muskat, M.: 1949, *Physical Principles of Oil Production*, McGraw-Hill, London.
- Raghavan, R. and Jones, J.: 1996, Depletion performance of gas-condensate reservoirs, *JPT*, 725–731.
- Saevareid, A., Whitson, C. H. and Fevang, Ø.: 1999, An engineering approach to measuring and modeling gas condensate relative permeabilities, Paper presented at the *1999 SCA Conference* held in Golden, CO, August 2–4, 1999.
- Standing, M. B.: 1975, Notes on relative permeability relationships, Proc., University of Trondheim, NTH, Norway.
- Stewart, G.: 1997, Personal communication, in: *IBC Conference on Optimisation of Gas Condensate Fields*.
- Whitson, C. H. and Fevang, Ø.: 1997, Generalized pseudopressure well treatment in reservoir simulation, In: *Proc. IBC Conference on Optimisation of Gas Condensate Fields*.